

## **A Study on Irradiation Hardening and Deformation Characteristics of Ion-irradiated bcc and fcc Metals by Using Nanoindentation Test**

Jae-Hoon Lee<sup>a</sup>, In-Sup Kim<sup>a</sup>, Sang-Chul Kwon<sup>b</sup>

<sup>a</sup> *Department of Nuclear and Quantum Engineering, Korea Advanced Institute of Science and Technology, 373-1, Gusong-dong, Yusong-gu, Daejeon 305-701, South Korea*

<sup>b</sup> *Korea Atomic Energy Research Institute, 150, Dukjin-dong, Yusong-gu, Daejeon 305-353, South Korea*

### **Abstract**

The nanoindentation test is carried out to evaluate irradiation hardening and deformation characteristics of ion-irradiated bcc and fcc metals. The specimens are irradiated at 60 °C up to the fluence of 0.15dpa and 1.5dpa by utilizing 8MeV Fe<sup>+4</sup> ions. The hardness values show depth dependent profiles from the irradiated specimen surface. In  $L/D$  and  $D$  plot, the pop-in phenomenon is able to estimate radiation defects at the peak displacement damage depth and irradiation hardening due to radiation-induced defects. The result of the hardness ratio increasing with doses means dose dependence of irradiation hardening in all specimens, before and after irradiation. The derivative of the load-to-depth ratio,  $d(L/D)/dD$ , is evaluated for the depth-dependent deformation characteristics in irradiated specimens. This profile shows that the depth of the peak plastic deformation is 0.01 – 0.02 times smaller than that of the peak displacement damage calculated by TRIM98 code and the peak value of the deformation parameter moves to the specimen surface with increasing doses.

### **1. Introduction**

Since the degradation of mechanical properties caused by high energy neutron irradiation in in-core nuclear reactor structural components is one of the critical issues for maintenance of structural integrity, the understanding of mechanical properties before and after irradiation is very important and meaningful. In general, if high energy neutrons generated by nuclear fission or fusion reactions are irradiated in metals, they will create various kinds of defects, resulting in irradiation-induced hardening accompanied by reduction in ductility and change of fracture mode from ductile to brittle fracture [1]. Further, the nature and type of those defects was known as much different depending on the crystal structure, namely, face-centered-cubic (fcc) and body-centered-cubic (bcc) crystal. As the results, the hardening behavior also might be

different according to the nature of the defects, which formed at each crystal structure. In this respect, the investigation of hardening behavior as a function of crystal structure is valuable for obtaining safe operation and extension of service life.

On the other hand, there exist some problems for studying the irradiation effects on metals using a neutron irradiation, for examples, the difficulties of the handling because of high radioactivity and of the controlling of temperature, flux and doses. For that reason, ion-irradiation techniques have been developed to study the microstructural characteristics and mechanical property changes with irradiation, instead of neutron irradiation. Over than four decades, ion irradiation techniques have been continuously developed to simulate the neutron irradiation effects on metals and to study the microstructure alteration depending on dose, dose rate and temperature [2]. Although ion irradiation techniques have been used to evaluate the mechanical properties of irradiated materials, however, they also have some shortages for measurement of bulk mechanical properties because the damaged layers induced by ion irradiation are extremely small (1~2 $\mu$ m). Thus, extreme care should be taken into account for use of evaluation of mechanical properties.

The nanoindentation test is one of the useful methods to correlate and to compare between microstructural evolution near the surface under ion irradiation and macroscopic mechanical properties [3], especially for non-destructive tests. Nanoindentation testing is able to measure hardness and load values of irradiated metals and alloys. The hardness and the load calculated with a specified method are neither physical quantities nor empirical ones. They represent a scale by themselves, allowing the comparison of materials. A comparison of the scales with each other and with other qualities of the material must be carried out empirically [4]. The hardness value usually means a resistance to plastic and elastic deformation in metals [5], and it also indicates the indirect evidence of material degradation. In this ways, the measurement of the hardness and load values would be a relatively good method to study the changes in deformation characteristics, before and after irradiation.

In the present work, the irradiation-induced hardening and deformation characteristics of various kinds of bcc and fcc metals have been studied after ion irradiation with different fluences and flux conditions. Nanoindentation test has been carried out to understand the irradiation hardening behavior and deformation characteristics as a function of crystal structure and indentation depth from the irradiated surface.

## **2. Experimental**

### *2.1 Material Preparation*

The materials in the present study are (i) bcc Fe (99.99%) single crystal and SA508 CL.3 steel and (ii) fcc Ni (99.994%) and Cu (99.99%) single crystals. The chemical compositions and

heat treatment condition of SA508 CL.3 steel are shown in table 1.

The specimens for the nanoindentation test were square plates with dimensions of 5mm×5mm×0.5mm. All the specimen surfaces for ion irradiation and nanoindentation measurement were mechanically polished up to a roughness of 1µm. Residual diamond particles embedded in the surface of samples were removed in ethanol after the mechanical polishing.

**Table 1** The chemical compositions and the heat treatments of SA508 CL.3 steel (in wt.%).

C	Mn	Ni	Mo	Cu	Al	P	S	Si	Cr	N	V	Fe
0.17	1.35	0.82	0.5	0.03	0.015	0.006	0.002	0.1	0.16	0.0055	0.004	Bal.

(HANJUNG, Ltd)

Heat Treatments:

Quenching at 880 for 8hr followed by water quench, and then tempering at 660 for 10.5hr followed by air cooled

## 2.2 Chemical Polishing

To remove scratches and deformation from fine grinding, all the specimens were chemically polished. Chemical polishing is a method for obtaining a polished surface by immersion in or swabbing with a suitable solution without need of the external electric current. The solutions used for chemical polishing of the specimens are shown in table 2 [6]. Fe and SA508 CL.3 steel were swabbed with the fresh solution at 25 for 4-10sec, and then flushed immediately with cold water. Ni and Cu were used at 25 for 1min.

**Table 2** The solution used for chemical polishing of bcc and fcc metals [6].

Material	Chemical polishing solution
SA508 CL.3 steel and Iron	80mL H <sub>2</sub> O <sub>2</sub> (30%) + 15mL Water + 5mL HF + 80mL H <sub>2</sub> O <sub>2</sub> (30%)
Copper	80mL H <sub>2</sub> SO <sub>4</sub> + 20mL HNO <sub>3</sub> + 1mL HCl + 55-60g CrO <sub>3</sub> + 200mL Water
Nickel	65mL Acetic Acid (ice-cooled) + 35mL HNO <sub>3</sub> + 0.5mL HCl

## 2.3 TRIM Simulation

TRIM98 code was used to determine the displacement damage depth, displacement per atom (dpa) dose and accelerator condition with 8MeV Fe ion. The calculated displacement energy of

Fe, Ni and Cu is 22, 24 and 19eV.

#### 2.4 Ion Irradiation

All specimens were irradiated with 1.6MV terminal voltage and 8MeV Fe<sup>+4</sup> ions to 0.15dpa and 1.5dpa using a Tandem Vande-Graaff accelerator (model: NEC 5SDH-2) at the Korea Institute of Geology and Mining (KIGAM). Beam homogeneity was achieved by the electric field scanning. Beam current was 250nA; flux was  $3.9 \times 10^{15}$  ions · m<sup>-2</sup> · sec<sup>-1</sup>; and fluence was  $4.24 \times 10^{18}$  ions · m<sup>-2</sup> at 0.15dpa and  $4.24 \times 10^{19}$  ions · m<sup>-2</sup> at 1.5dpa. The irradiation period was 1086sec for 0.15dpa and 10860sec for 1.5dpa. The beam diameter was 10mm (Quadrangle Beam). The irradiation chamber was kept in a vacuum of 10<sup>-6</sup> Torr and the irradiation temperature was not over 60 °C.

#### 2.5 Nanoindentation Continuous Stiffness Measurement (CSM) Test

Nanoindentation CSM test was performed in a Berkovich indenter and used to measure the load and hardness profile through the depth of bcc and fcc metals. In this investigation, the indentation load was not fixed, however the indentation depth was fixed at 500 nm for SA508 CL.3 steel and 1000 nm for other specimens. Since the thickness of the ion-beam modified layer is very shallow, in the range of between 1200 nm and 2400 nm, the effect of the underlying unirradiated substrate becomes significant as the indenter approaches the depth of the ion range. In this report, it was found that the hardness value at 350 nm indentation depth is a good representation of the surface hardness for comparison purposes with the least surface and substrate effects as described in the results section. The elastic effects from both the modified layer and the supporting materials have been discussed by Bhattacharya and Nix [7]. To accommodate the effects of the substrate, indenter tip geometry, and other subsurface artifacts, hardness values can be normalized to the unirradiated material hardness [8]. Uncertainty in the indenter displacement increases at larger load speed especially at the beginning stage of its contact on the surface of the specimen, while vibration of the indentation machine can affect load-displacement results at lower speed. The loading rate was set at 0.05sec<sup>-1</sup>. To avoid any effects from grain boundaries, the test regions were carefully chosen.

### 3. Results and Discussion

#### 3.1 Damage Depth Profiles

Figure 1 shows the results of TRIM98 simulation for the displacement damage depth profile in the irradiated area. It is shown that the peak damage depth appears at around 1600 nm in Fe, 1500 nm in Ni, and 1800 nm in Cu. This peak damage depth is related with radiation defects generated by irradiation. Victoria *et al.* showed that a majority of the defect clusters observed in

fcc Ni and Cu were stacking fault tetrahedra (SFT), while small interstitial loops formed the major fraction of defects in bcc Fe and SA508 CL.3 steel. In terms of the type of defects, these observations indicate that in low stacking fault energy (SFE) fcc Ni and Cu, the majority of defects observed are SFTs, while, as the SFE increases in bcc Fe and SA508 CL.3 steel, small interstitial loops are the main result of the irradiation with either ions or neutrons [8, 9].

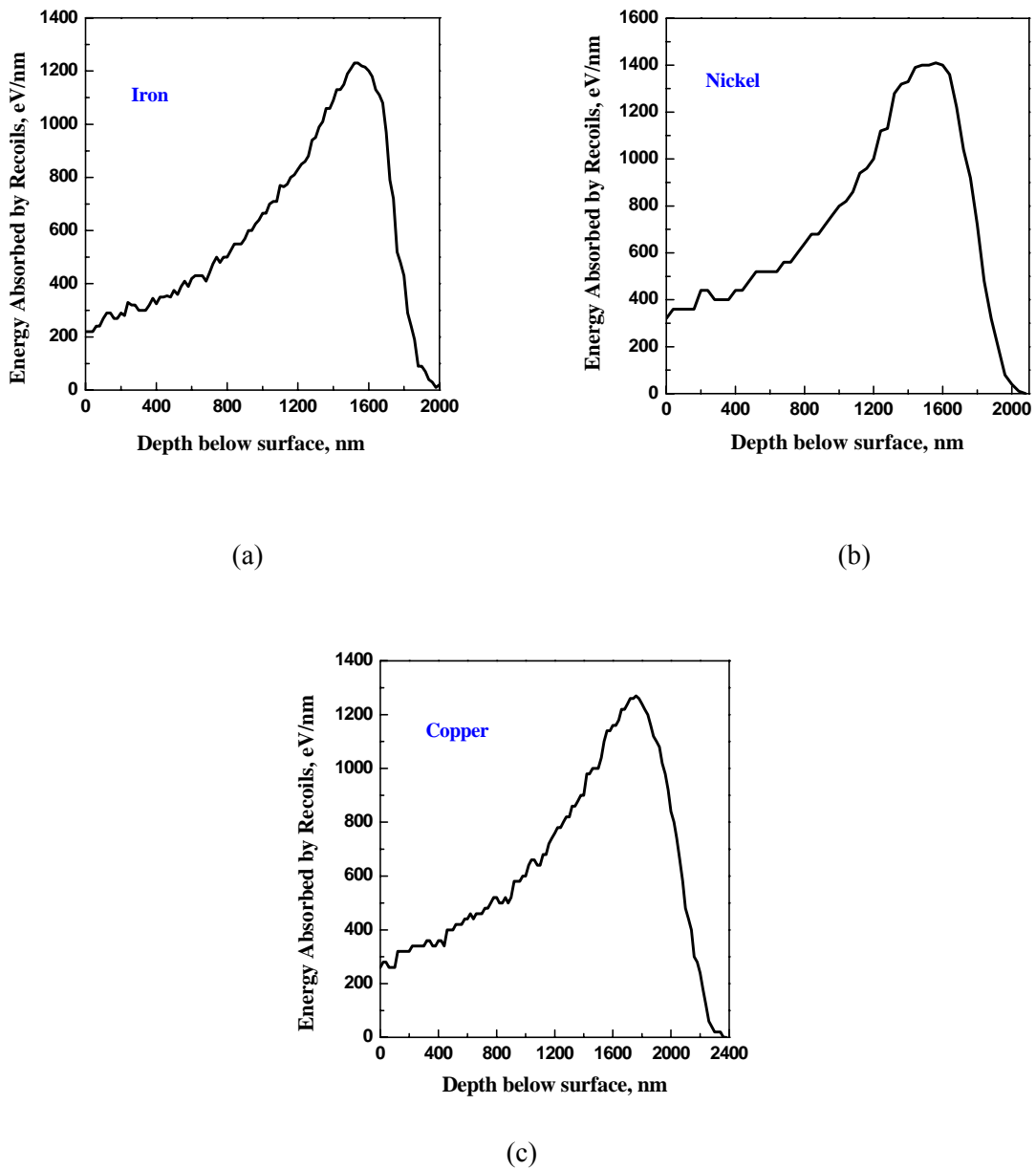
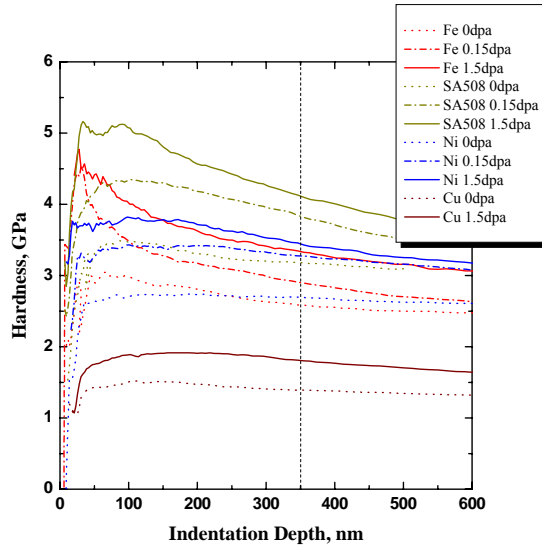


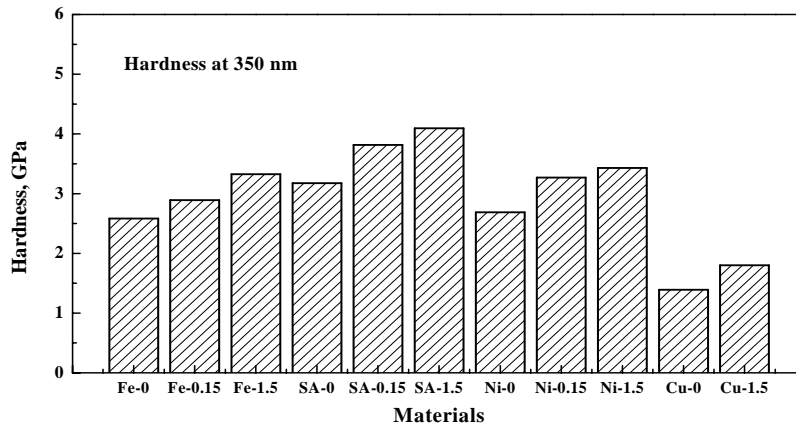
**Figure 1** The calculated depth distribution of displacement damage in iron (a), nickel (b) and copper (c) by the TRIM98 simulation of the energy profile from 8MeV Fe ion.

### 3.2 Irradiation Hardening

Figure 2 compares hardness data for 8MeV Fe<sup>+4</sup> ion beam irradiated specimens, all irradiated at 60 °C or below. This figure shows the indentation depth dependence of hardness value.



(a)



(b)

**Figure 2** Hardness values as a function indentation depth for Fe, SA508 CL.3 steel, Ni and Cu both un-irradiated and irradiated with 8MeV Fe<sup>+4</sup> ions to 0.15dpa and 1.5dpa at 60 °C or below (a) and comparison of hardness values at 350 nm depth (b).

Typically, the stress field surrounding the indenter tip extends to about 7 times the penetration depth. Thus hardness values at 350 nm depth have been used as representative values for comparison in this report [10]. Each hardness value through depth of the unirradiated materials is almost saturated in 2.5 GPa in Fe, 3.2 GPa in SA508 CL.3 steel, 2.7 GPa in Ni, and 1.4 GPa in Cu. In ion irradiation, bcc SA508 CL.3 steel showed the highest hardness value, 3.8 GPa at 350 nm in 0.15dpa and 4.1 GPa at 350 nm in 1.5dpa decreasing with getting deeper depth. Hardness value of bcc Fe with a increase in hardness (2.9 GPa at 350 nm in 0.15dpa and 3.4 GPa at 350 nm in 1.5dpa) steep decreases during increasing depth. On the other hand, fcc Ni (3.3 GPa at 350 nm in 0.15dpa and 3.5 GPa at 350 nm in 1.5dpa) and Cu (1.8 GPa at 350 nm in 1.5dpa) are on the moderate decrease of hardness value with depth.

Figure 3 shows hardness values of the irradiated specimens normalized to the unirradiated specimen hardness value. The peak value for hardness ratio appears at 15 – 30 nm depth. The depth at the peak hardness ratio of irradiated specimens is 0.01 – 0.02 times the depth at peak displacement damage. Also, the highest hardness ratios are found to be approximately irradiated specimens at 1.5dpa. The hardness ratio of Ni and SA508 CL.3 steel is larger than one of Fe at 0.15dpa. A gradual decrease in hardness ratio was evident beyond 350 nm indentation depth caused by greater influence of the underlying unirradiated substrate. This peak value for hardness ratio is depending on radiation defects at peak displacement damage.

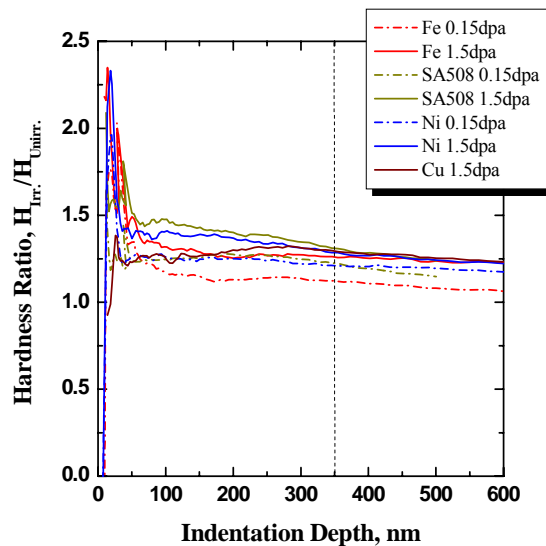


**Figure 3** Hardness values of the irradiated specimens normalized to the unirradiated specimen hardness value.

Irradiation hardening is related with the dislocation movement. Notice that there are two

contributions to the increase of hardening of the irradiated materials. On the one hand, the dislocation generated and grown during irradiation will give rise to the stress required to start a dislocation moving on its glide plane. This irradiation hardening, a source hardening, is generated in bcc and fcc metals. Second, the moving dislocation in the crystal will be pinned down by the defects, such as SFTs, interstitial loops, vacancies, and black dots produced during irradiation. The pinned dislocation will increase the irradiation hardening, a friction hardening, in all irradiated materials.

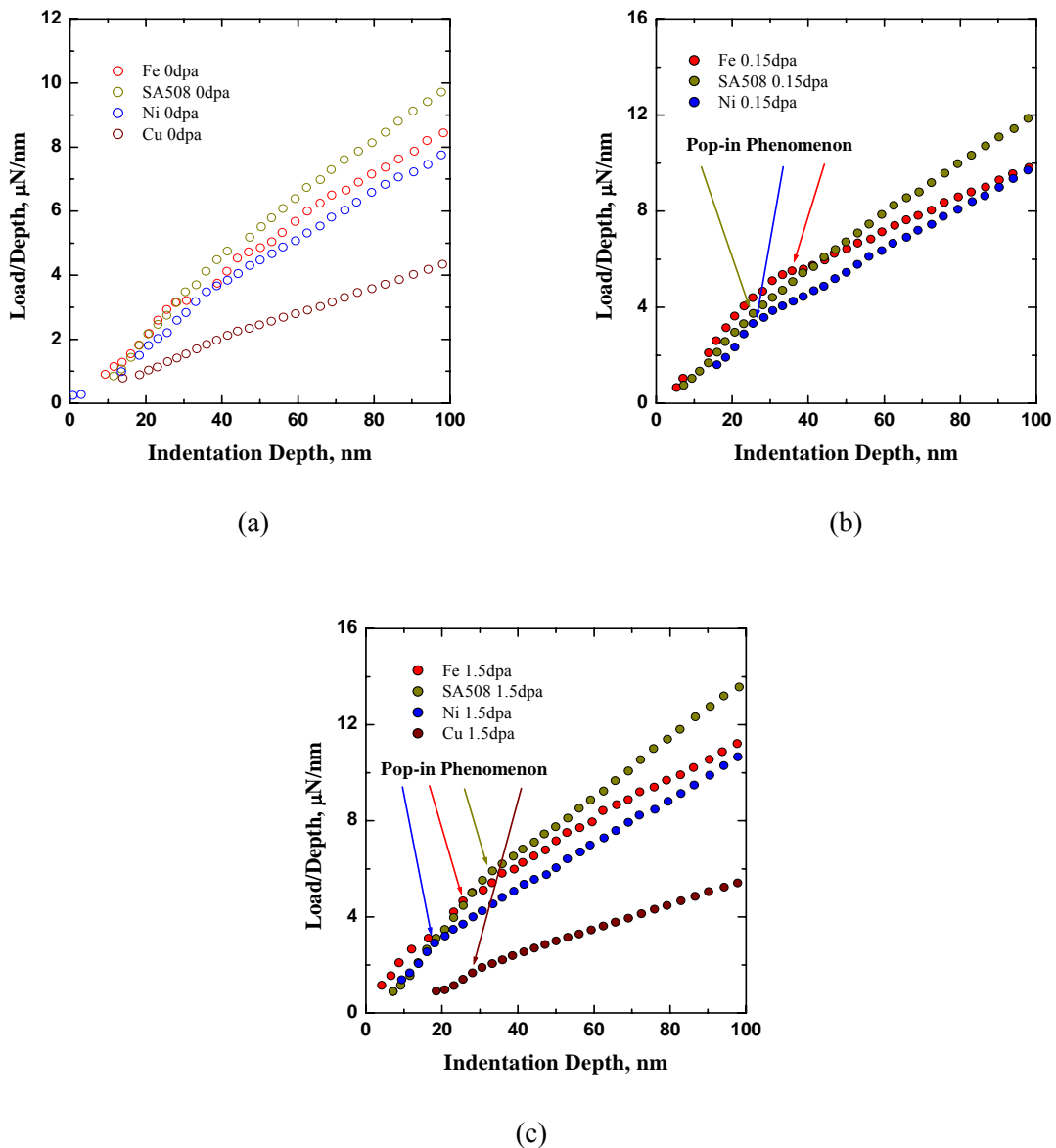


**Figure 4** Typical load/depth – depth plots in unirradiated specimens (a) together with that of bcc and fcc materials for irradiations at 60 to doses of 0.15dpa (b) and 1.5dpa (c).

Typical *Load/Depth – Depth* plots in bcc and fcc materials for irradiations at 60 °C to doses of 0.15dpa and 1.5dpa are given in figure 4 together with that of unirradiated specimens. The unirradiated specimens show good linear relation between  $L/D$  and  $D$  through the measured range in figure 4 (a). In the irradiated bcc and fcc metals with 0.15dpa and 1.5dpa, however, the plots does not show linearity. In this figure 4 (b), the gradient of the plot in irradiated specimens with 0.15dpa increases with increasing dose at shallow subsurface region less than about 35 nm in Fe and 25 nm in SA508 CL.3 and Ni in depth. Also when irradiated at 1.5dpa condition, the graph's slope increases with the rising dose. And the value is same with the case of 28 nm in Fe, 33 nm in SA508 CL.3, 20 nm in Ni, and 30 nm in Cu.

The sudden penetration described above is similar to so called pop-in phenomenon of hard-coated materials, in which a soft substrate is coated with a hard layer. The pop-in phenomenon occurs when the plastically deformed region formed around indenter tip reaches the film-substrate interface. Based on these studies, the present results can be interpreted as following. The subsurface layer where Fe ions cause direct damage is hardened and when the plastic zone formed around the indenter tip reaches the interface of the damaged layer and the undamaged substrate, which is likely to about 2  $\mu\text{m}$  in Fe and Ni and 2.4  $\mu\text{m}$  in Cu in depth, the pop-in occurs. It is reasonable, therefore, to estimate the average hardness of the damage layer from the *Load/Depth – Depth* plot before pop-in movement.

### 3.3 Dose Dependence of Radiation Hardening

Figure 5 shows dose dependence of hardening of the damaged layer at 350 nm in bcc and fcc metals for 8MeV  $\text{Fe}^{+4}$  ion irradiation at 60 °C. This figure shows that the Fe metal's hardness ratio increases faster than the others' hardness ratio with the same irradiated doses, and radiation hardening is proportional to the irradiation dose.

Generally, the increase in the hardness ratio with increasing dose is considered to occur due to the presence of irradiation-induced vacancy clusters and loops which are assumed to act as barriers to mobile dislocations in the glide plane. In this model, called the dispersed-barrier hardening model, the mobile dislocations under the action of an applied stress are supposed to overcome these barriers either by bowing out between or cutting through these clusters and loops. The increase in the stress necessary to drive the dislocations through these obstacles is then related to the irradiation dose by assuming that each collision produces one vacancy cluster and loop. On the basis of these considerations, the model predicts that the irradiation-induced hardening should be proportional to the square root of the irradiation dose, that is, the radiation hardening depends on the irradiation dose. It is of interest to examine some basic aspects of the concept of irradiation hardening under cascade damage conditions [11].

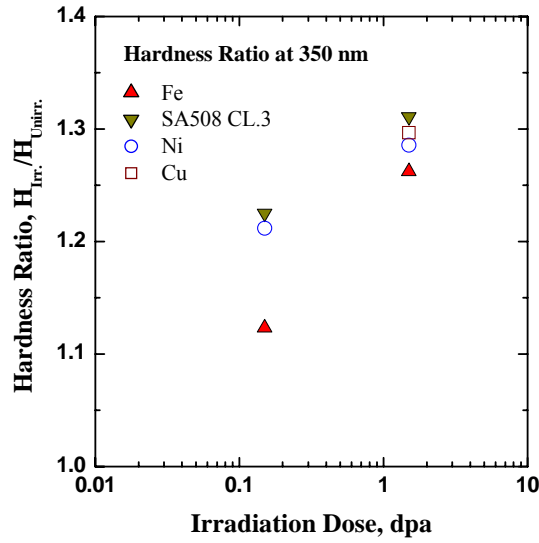


**Figure 5** Dose dependence of the hardening of the damaged layer at 350 nm in bcc and fcc metals for 8MeV Fe<sup>+4</sup> ion irradiation at 60 °C.

### 3.4 Plastic and Elastic Deformation

Figure 6 shows the indentation depth dependence of the derivative value of the load-to-depth ratio,  $d(L/D)/dD$ . The depth profile of this parameter describes the depth dependence of plastic and elastic deformation. The peak value for this deformation parameter appeared at 8 – 25 nm depth in Fe (a), 10 – 30 nm depth in SA508 CL.3 steel (b), 15 – 25 nm depth in Ni (c), and 25 – 30 nm depth in Cu (d). Because the effect of elastic deformation should not be considered except for estimating very low loading rate, the derivative value of the load-depth can be simply thought of plastic deformation. The depth at the peak plastic deformation of bcc and fcc metals is 0.01 ~ 0.02 times the depth at peak displacement damage. This can be partly explained by the fact that the shearing probability is much larger near the surface than in the bulk, owing to the elastic dipole interaction in the bulk between dislocation loops of opposite character, or between loops of vacancies or interstitials [12].

The characteristic thing is that the peak value of the deformation parameter moves to the specimen surface with increasing irradiation. This phenomenon can be verified by figure 7. The peak value of bcc Fe and SA508 CL.3 steel moves more to the surface than one of fcc Ni and Cu metals doing at 0.15dpa but at 1.5dpa, it move less to the surface than the peak value of fcc specimens. We can explain this at this way.  $d(L/D)/dD$  is the characterizing plastic and elastic deformation. So the peak value for this deformation parameter is related with the density of radiation defects at peak displacement damage. When radiation defects are generated by

irradiation, the peak value moves to the surface and as the more radiation defects generated it moves to the surface more.

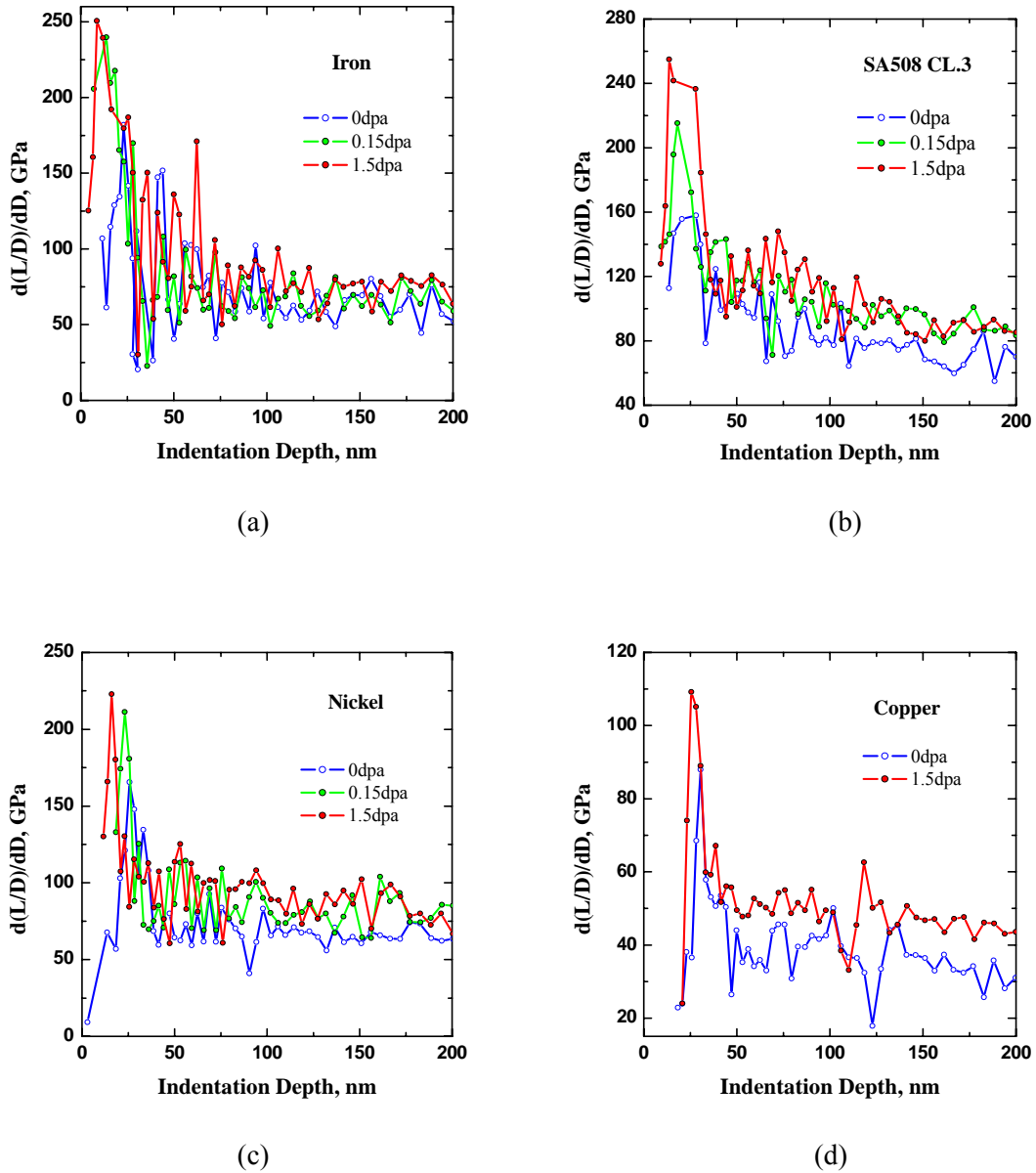


**Figure 6** Derivative value of  $(L/D)$  as a function of indentation depth  $(D)$  in Fe (a), SA508 CL.3 steel (b), Ni (c), and Cu (d) both un-irradiated and irradiated with 8MeV  $Fe^{+4}$  ions to 0.15dpa and 1.5dpa at 60 or below.

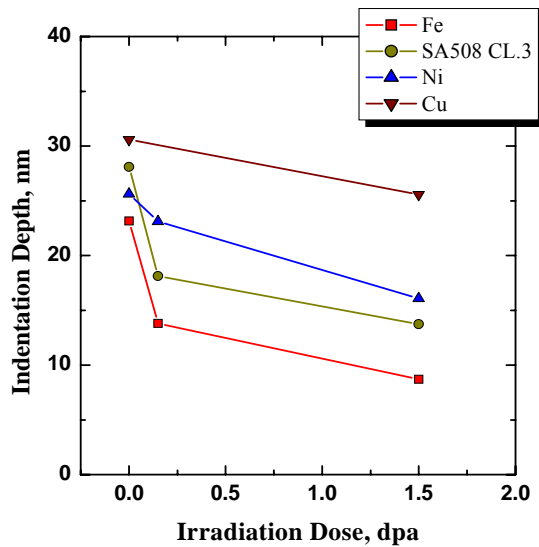


**Figure 7** Irradiation dose vs. indentation depth profile of the peak value for  $d(L/D)/dD$  in fcc and bcc materials both un-irradiated and irradiated with 8MeV  $Fe^{+4}$  ions to 0.15dpa and 1.5dpa at 60 .

#### 4. Conclustions

The nanoindentation CSM technique is able to measure hardness and load values of bcc and fcc metals for non-destructive tests. The measurement of the hardness and load values as a function of depth from the surface would be good method to investigate the changes in irradiation hardening and deformation characteristics, before and after irradiation. The main conclusions are as follows:

- (1) In non-irradiation, a hardness value is almost saturated with depth in bcc and fcc metals, but in ion irradiation the hardness value steep decreases with depth in bcc metals and moderate decreases with depth in fcc metals. A depth at the peak hardness ratio is 0.01 – 0.02 times the depth at the peak displacement damage due to radiation-induced defects.
- (2) In  $L/D$  and  $D$  plot, the pop-in phenomenon is able to evaluate radiation defects at the peak displacement damage depth and irradiation hardening due to radiation defects. When the plastic zone formed around the indenter tip reaches the interface of the damaged layer and the undamaged layer, which is likely to about 2  $\mu m$  in Fe and Ni and 2.4  $\mu m$  in Cu in depth, the pop-in phenomenon occurs.
- (3) The result of the hardness ratio increasing with doses means dose dependence of irradiation hardening in bcc and fcc metals. The Fe metal's hardness ratio increases faster than the others' hardness ratio with the same irradiated doses, and irradiation hardening is

proportional to the irradiation dose.

- (4) The depth profile of  $d(L/D)/dD$  describes the depth dependence of deformation characteristics. The depth of the peak plastic deformation is 0.01 – 0.02 times smaller than that of the peak displacement damage calculated by TRIM code.
- (5) A peak value of the deformation parameter moves to the specimen surface with increasing irradiation. The peak value of bcc Fe and SA508 CL.3 steel moves more to the surface than one of fcc Ni and Cu metals doing at 0.15dpa but at 1.5dpa. The peak value for this deformation parameter is related with the density of radiation defects at the peak displacement damage. When radiation defects are generated by irradiation, the peak value moves to the surface and as the more radiation defects generated it moves to the surface more.

### References

- [1] A. Iwase, T. Hasegawa, Y. Chimi, T. Tobita, N. Ishikawa, M. Suzuki, T. Kambara, S. Ishino, Nucl. Instr. and Meth. B 195 (2002) 309-314.
- [2] Naoto Sekimura, Toru Kamada, Yohei Wakasugi, Taira Okita, Yoshio Arai, J. of Nucl. Mater. 307-311 (2002) 308-311.
- [3] S.J. Zinkle, W.C. Oliver, J. Nucl. Mater. 141-143 (1986) 548.
- [4] J. H. Westbrook and H. Conrad, “The Science of Hardness Testing and Its Research Applications”, American Society for Metals, p.17-19 (1973).
- [5] George E. Dieter, “Mechanical Metallurgy,” McGraw-Hill, p.325-337 (1986).
- [6] George F. Vander Voort, “Metallography Principles and Practice”, McGraw-Hill Book Company, p.552-561 (1984).
- [7] A. K. Bhattacharya and W. D. Nix, Int. J. Solids Structures, 24 (1988) 1287.
- [8] Jun-Hyun Kwon, Sang-Chul Kwon, Jun-Hwa Hong, “Multiscale Modeling of Radiation Hardening in Pressure Vessel Steels”, Proc. KNS Autumn Meeting (2003).
- [9] M. Victoria, N. Baluc, C. Bailat, Y. Dai, M.I. Luppó, R. Schaublin, B.N. Singh, J. Nucl. Mater. 276 (2000) 114-122.
- [10] E.H.Lee, G.R.Rao, L.D.Huun, P.M.Rice, M.B.Lewis, S.W.Cook, K.Farrell, and L.K.Mansur, Proceeding of the symposium on materials for spallation neutron sources, pp.57-pp.65, 1997 TSM annual meeting.
- [11] B. N. Singh, A. Horsewell, P. Toft, D. J. Edwards, J. Nucl. Mater. 224 (1995) 131-140.
- [12] K. Nordlund, J. Keinonen, M. Ghaly & R. S. Averback, NATURE, VOL 398, 4 MARCH 1999.